Anti-Candida Cassane-Type Diterpenoids from the Root Bark of Swartzia simplex

ARTICLE *in* JOURNAL OF NATURAL PRODUCTS · DECEMBER 2015

Impact Factor: 3.8 · DOI: 10.1021/acs.jnatprod.5b00744

JOURNAL OF NATURAL PRODUCTS

Article

pubs.acs.org/jnp

Anti-*Candida* Cassane-Type Diterpenoids from the Root Bark of *Swartzia simplex*

Quentin Favre-Godal,[†] Stephane Dorsaz,[‡] Emerson F. Queiroz,[*,†] Laurence Marcourt,[†] Samad N. Ebrahimi,[§] Pierre-Marie Allard,[†] Francine Voinesco,[⊥] Matthias Hamburger,[○] Mahabir P. Gupta,[#] Katia Gindro,[⊥] Dominique Sanglard,[‡] and Jean-Luc Wolfender[†]

[†]School of Pharmaceutical Sciences, EPGL, University of Geneva, University of Lausanne, 30 quai Ernest-Ansermet, CH-1211 Geneva 4, Switzerland

[‡]Institute of Microbiology, University of Lausanne and University Hospital Center, Rue du Bugnon 48, CH-1011 Lausanne, Switzerland

[§]Department of Phytochemistry, Medicinal Plants and Drugs Research Institute, Shahid Beheshti University, G. C., Evin, P.O. Box 19835-389, Tehran, Iran

[⊥]Agroscope, Institute for Plant Production Sciences (IPS), Mycology and Biotechnology, Route de Duiller 50, P.O. Box 1012, CH-1260 Nyon, Switzerland

[○]Division of Pharmaceutical Biology, Department of Pharmaceutical Sciences, University of Basel, Klingelbergstrasse 50, CH-4056 Basel, Switzerland

[#]Center for Pharmacognostic Research on Panamanian Flora (CIFLORPAN), University of Panama, P.O. Box 0824-00172, Panama City, Panama

Supporting Information

ABSTRACT: A dichloromethane extract of the roots from the Panamanian plant *Swartzia simplex* exhibited a strong antifungal activity in a bioautography assay against a genetically modified hypersusceptible strain of *Candida albicans*. At-line HPLC activity based profiling of the crude extract enabled a precise localization of the antifungal compounds, and dereplication by UHPLC-HRESIMS indicated the presence of potentially new metabolites. Transposition of the HPLC reversed-phase analytical conditions to medium-pressure liquid chromatography (MPLC) allowed an efficient isolation of the major constituents. Minor compounds of interest were isolated from the MPLC fractions using semipreparative HPLC. Using this strategy, 14 diterpenes (**1**−**14**) were isolated, with seven (**5**−**10**, **14**) being new antifungal natural products. The new structures were elucidated using NMR spectroscopy and HRESIMS analysis. The absolute configurations of some of the compounds were elucidated by electronic circular dichroism spectroscopy. The antifungal properties of these compounds were evaluated as their minimum inhibitory concentrations in a dilution assay against both hypersusceptible and wild-type strains of *C. albicans* and by assessment of their antibiofilm activities. The potential cytological effects on the ultrastructure of *C. albicans* of the antifungal compounds isolated were evaluated on thin sections by transmission electron microscopy.

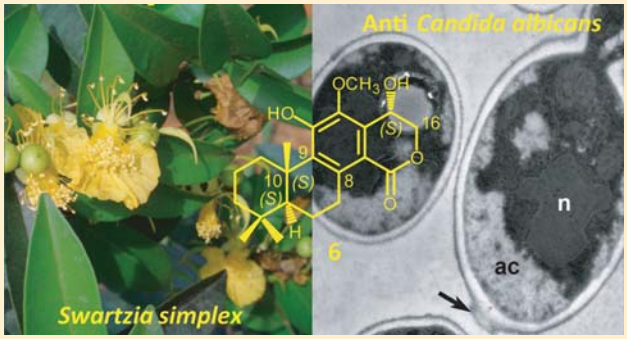

There is an increasing awareness worldwide of the high morbidity and mortality rates among different groups of human patients caused by fungal infections.[1] One reason is the increase of drug resistance in fungal pathogens that compromises the efficacy of the limited number of therapeutic agents. Even the activity of echinocandins, the newest generation of antifungal drugs, is gradually declining, due to the occurrence of different resistance mechanisms.[2] The resistance of some microorganisms is also due to their capacity to form biofilms. Biofilms are structured microbial communities that are attached to a surface, which may induce pathogenicity through various mechanisms and exhibit enhanced resistance to antifungal agents and protection from host defenses.[3,4] This could result in the incapacity to cure an infection due to the high concentrations of required antibiotics, which may become toxic.[5] These facts indicate the strong need to discover new natural products (NPs) that potentially can become efficient antimicrobial agents against planktonic cells or biofilms with higher efficiencies, lower toxicities, or new modes of action.[6] In

Received: August 19, 2015

DOI: 10.1021/acs.jnatprod.5b00744
J. Nat. Prod. XXXX, XXX, XXX−XXX

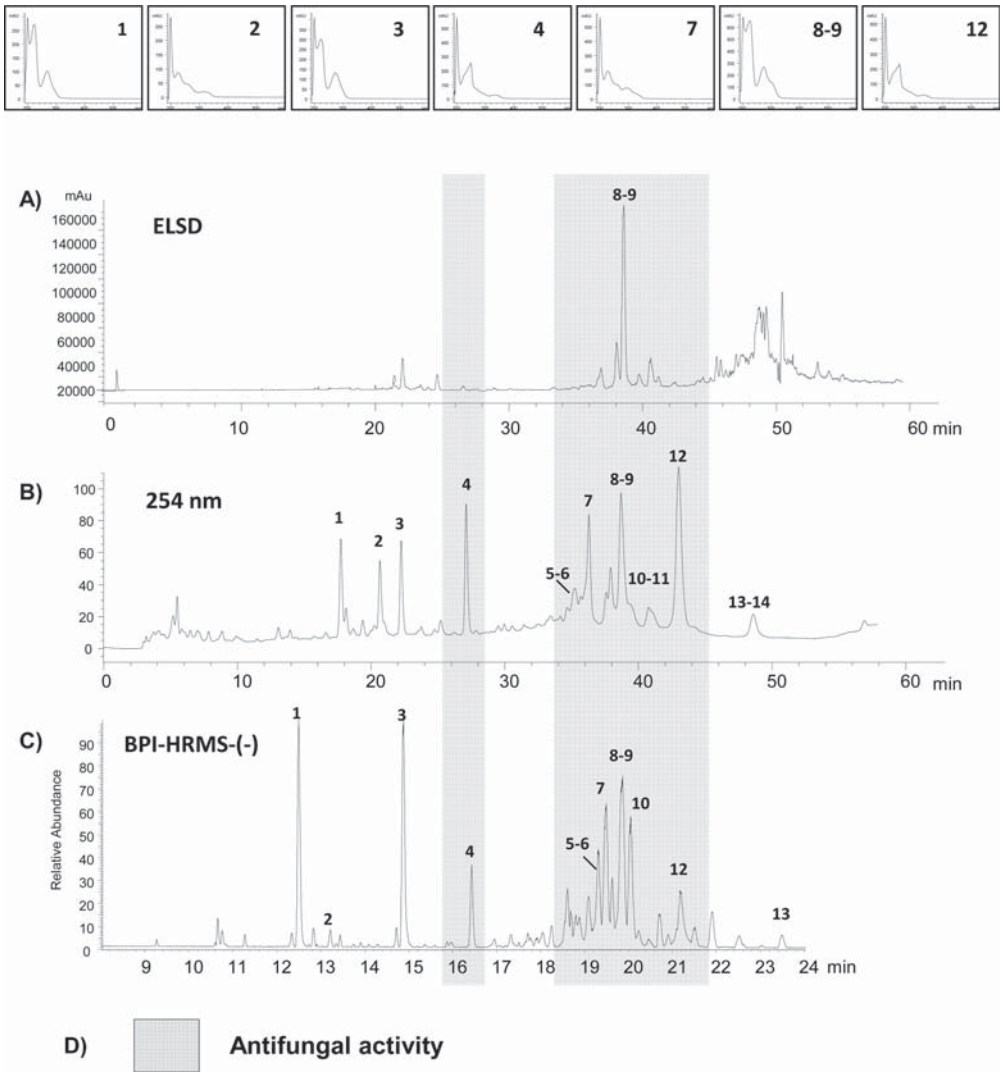

Figure 1. (A and B) HPLC-PDA-ELSD analysis of the CH_2Cl_2 extract of the roots of *S. simplex*. (C) Negative ion (NI)-ESI base peak ion (BPI) trace of the UHPLC-Orbitrap-MS analysis of the root CH_2Cl_2 extract of *S. simplex*. (D) Gray zones indicate antifungal activity revealed by bioautography after microfractionation.

this context, polyenes and echinocandins of microbial origin are recognized as important therapeutic classes of antifungals.[7]

The genus *Swartzia* belongs to the tribe Swartzieae of the family Leguminosae and consists of about 180 species distributed in tropical America.[8] Only a single genus, called *Bobgunnia*, has been described in Africa.[9] Metabolites isolated from *Swartzia* species have been reported to have antimicrobial and molluscicidal activities.[10−14] *Swartzia simplex* (Sw.) Spreng. is a tree or less frequently a shrub that occurs mostly in rain forests, mangroves, and coniferous forests and sometimes has been reported from dry forests, xeric scrublands, and Caribbean shrub lands.[15] An aqueous extract of this plant is used traditionally in Panama to treat wounds.[16] A crude ethanolic extract was reported to exhibit a wide spectrum of antibacterial and antifungal activities.[15] Previous studies on this species have led to the isolation of triterpenoids and molluscicidal saponins.[17]

The present study deals with the isolation and structure elucidation of the antifungal compounds from the dichloromethane extract of the root bark of *S. simplex*. The compounds obtained were evaluated for their antifungal activities against planktonic cells of *Candida albicans* in a microplate dilution assay and for their antibiofilm activities. The cytological effects of the most potent antifungal compound were examined by transmission electronic microscopy (TEM).

■ RESULTS AND DISCUSSION

In a preliminary screening procedure, the CH_2Cl_2 root bark extract of *S. simplex* showed significant antifungal activity in a bioautography assay using a genetically modified strain of *C. albicans* (Figure S1, Supporting Information). This strain has been reported to be highly susceptible and suitable for a better detection sensitivity.[18] The same crude extract did not show activity against a *C. albicans* wild-type strain, thus indicating the probable presence of the active constituents only in low concentration levels. HPLC-PDA-evaporative light scattering detection (ELSD) analysis revealed a very complex mixture of metabolites. The majority of the compounds detected displayed similar UV spectra, suggesting the presence of metabolites with related structures. ELSD showed few major LC peaks

DOI: 10.1021/acs.jnatprod.5b00744
J. Nat. Prod. XXXX, XXX, XXX−XXX

Chart 1

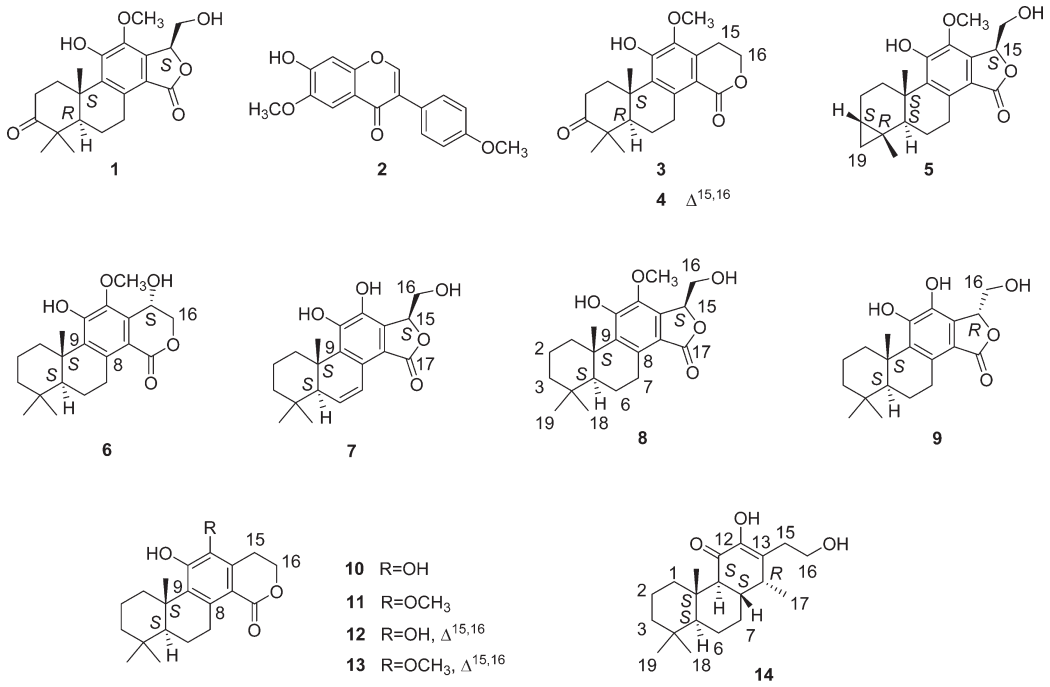

corresponding to these metabolites (t_R 38−39 min), suggesting the presence of only some major constituents (Figure 1).

In order to localize the compounds responsible for the antifungal activity, the crude extract of *S. simplex* roots was subjected to semipreparative high-pressure liquid chromatography (HPLC) microfractionation on a small size using a high-resolution C_{18} column (250 × 10 mm i.d.).[18] The amount injected (25 mg) was chosen to allow a satisfactory detection by bioautography after microfractionation, and this yielded 50 fractions of 10 mL each. The gradient used for this separation was transferred geometrically from the analytical HPLC conditions of the metabolite profiling (Figure 1A) by applying a gradient transfer method to ensure similar selectivity.[19,20]

This procedure provided a high-resolution separation of the crude extract constituents, and most microfractions corresponded to single LC peaks. Bioautography with the hypersusceptible strain of *C. albicans* was performed directly on the microfractions previously transferred to the thin-layer chromatography (TLC) plate without any further elution step. Correlation of all bioautography results with the HPLC profiles enabled the identification of the LC peaks responsible for the antifungal activity (peaks at t_R 27 min and between 34 and 52 min) (Figure 1).

Dereplication of the metabolites eluting in the active zones was performed by complementary UHPLC-high-resolution mass spectrometry (HRESIMS) metabolite profiling of the crude extract in both the positive (PI) and negative (NI) electrospray ionization (ESI) modes (Figure 1C). A peak list of the relevant features (m/z at a given t_R; Table S1, Supporting Information) was compared to a comprehensive list of all the molecular formulas of chemical constituents reported in the *Swartzia* genus extracted from the *Dictionary of Natural Products* database.[21] This led to the tentative identification of 23 compounds within a 3 ppm tolerance (Table S1, Supporting Information). For all these compounds, molecular formulas were proposed based on exact mass determination within a 3 ppm range and isotopic pattern similarity and by applying heuristic filters.[22]

The first zone of bioactivity corresponded to peak 4 (t_R 16.4 min UHPLC; $C_{21}H_{24}O_5$; 0.25 ppm in PI; Table S1, Supporting Information), which was identified tentatively as swartziarboreol B.[23] In the second zone of bioactivity (t_R 18.5−24 min UHPLC) several peaks were overlapped. Four of these were dereplicated as swartziarboreol A or its isomers (peak 5; t_R 18.67 min UHPLC; $C_{21}H_{26}O_5$; 0.25 ppm in PI), swartziagenin (t_R 20.64 min UHPLC; $C_{30}H_{48}O_4$; −1.86 ppm in NI),[24] 15,16-dihydroswartziarboreol C (peak 11; t_R 21.88 min UHPLC; $C_{21}H_{28}O_4$; 0.76 ppm in PI),[25] and swartziarboreol C (peak 13; t_R 23.46 min UHPLC; $C_{21}H_{26}O_4$; 0.49 ppm in PI). Interestingly, one additional feature was assigned to 11,12-dihydroxy-8,11,13,15-cassatetraen-16,17-olide (peak 12; t_R 21.14 min UHPLC; $C_{20}H_{24}O_4$; 0.40 ppm in PI). This compound was previously postulated in *Swartzia langsdorffii* but has not been isolated.[25] Numerous other features in these chromatographic zones were related to metabolites not described in the *Swartzia* genus. The molecular formulas indicated the presence of structural analogues of *Swartzia* cassane diterpenes. On the basis of this preliminary information, the isolation of the antifungal agents and the compounds that were not yet reported was undertaken.

To fully characterize the metabolites of interest and quantify their antifungal effects, the active compounds were isolated at the milligram scale by reversed-phase medium-pressure liquid chromatography (MPLC) and semipreparative HPLC. A direct transfer of the analytical HPLC conditions to MPLC using the same reversed-phase material provided a rational and efficient fractionation of 7.13 g of the crude CH_2Cl_2 extract.[26] This resulted in the isolation of 14 pure compounds (**1**−**14**). Thus, the structures of six compounds dereplicated were confirmed unambiguously, and sufficient quantities were obtained for further antifungal dilution assays. Their absolute configurations were established by electronic circular dichroism (ECD)

DOI: 10.1021/acs.jnatprod.5b00744
J. Nat. Prod. XXXX, XXX, XXX−XXX

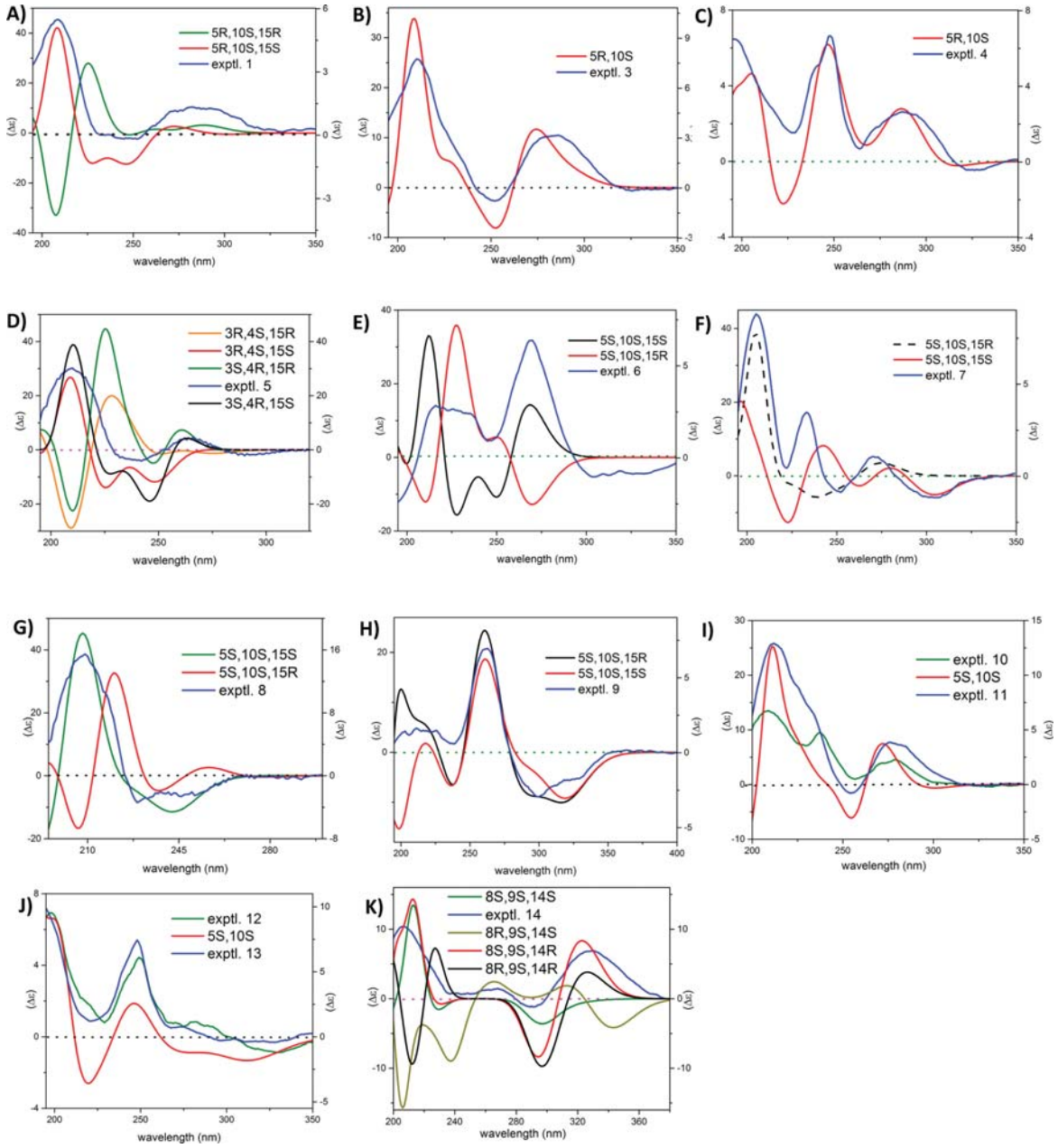

Figure 2. Comparison of experimental and calculated ECD spectra for the possible stereoisomers of **1** and **3**−**14**. Calculated spectra were obtained by using TDDFT at the B3LYP/6-31G** level of theory in MeOH.

spectroscopy since they were not previously reported. These compounds are swartziarboreol E (**1**),[23] swartziarboreol A (**3**),[23] swartziarboreol B (**4**),[23] 15,16-dihydroswartziarboreol C (**11**),[25] 11,12-dihydroxy-8,11,13,15-cassatetraen-17,16-olide (**12**),[25] and swartziarboreol C (**13**).[23] In addition afrormosine (**2**)[23] was also identified, although it could not be dereplicated in the extract. As expected from the dereplication, the purification also afforded seven new cassane-type diterpenes described below, namely, **5**−**10** and **14**. Their full identifications were performed de novo based on nuclear magnetic resonance (1D and 2D NMR) and HRESIMS experiments.

On the basis of the UHPLC-HRESIMS data (*m*/*z* 375.1803 $[M + H]^+$, $C_{21}H_{26}O_6$) and a cross search for molecular formulas previously reported in the genus *Swartzia,* compound **1** was dereplicated as either swartziarboreol D or swartziarboreol E (Table S1, Supporting Information). The ^1H and ^{13}C NMR chemical shifts of **1**, isolated as an amorphous solid, confirmed unambiguously that it is swartziarboreol E.[23] The characteristic features were signals for three methyls at δ_C 28.3, 20.3, and 19.3 (C-18, C-19, and C-20, respectively), one oxygenated methyl at δ_C 60.7 (C-21), two carbonyls at δ_C 220.4 and 164.9 (C-3 and C-17, respectively), one oxygenated methine at δ_C 80.3 (C-15), and one oxygenated methylene at δ_C 62.2 (C-16), in contrast to the cyclic methylene (C-16) of a dihydropyran unit as found in swartziarboreol D.[23]

The partial configuration of **1** at C-5 and C-10 has been established previously by comparison of the optical rotation as 5*R*, 10*S*, while the configuration of C-15 was not determined.[23] In order to fully establish the absolute configuration of swartziarboreol E (**1**), the ECD spectrum was measured and

DOI: 10.1021/acs.jnatprod.5b00744
J. Nat. Prod. XXXX, XXX, XXX−XXX

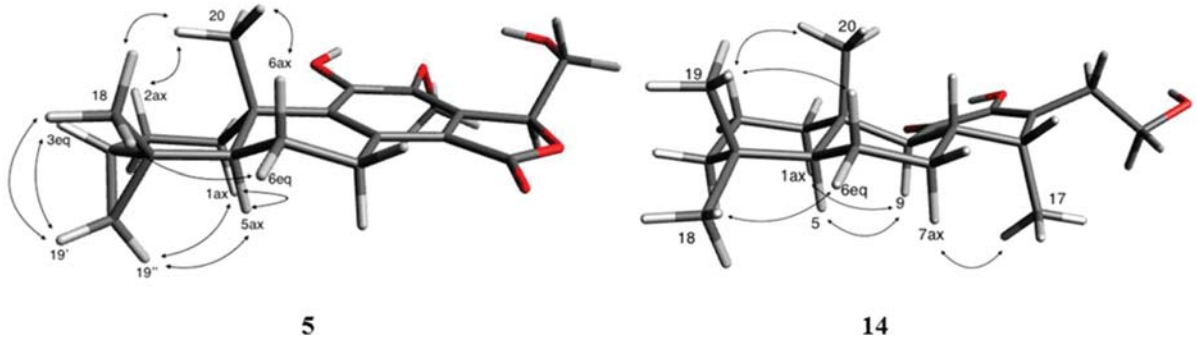

5 14

Figure 3. Key NOESY correlations of DFT-optimized structure of the 3*S*,4*R*,5*S*,10*S*,15*S* stereoisomer of compound **5** and the 5*S*,8*S*,9*S*,10*S*,14*R* stereoisomer of compound **14**.

Table 1. ^{13}C NMR Data for Compounds 5−10, 12, and 14 (125.71 MHz, MeOD, δ in ppm)

position	5	6	7	8	9	10	12	14
1	31.5, CH_2	37.1, CH_2	37.4, CH_2	37.2, CH_2	37.0, CH_2	37.6, CH_2	37.1, CH_2	41.2, CH_2
2	20.9, CH_2	20.4, CH_2	20.2, CH_2	20.3, CH_2	20.1, CH_2	20.4, CH_2	19.9, CH_2	19.5, CH_2
3	19.5, CH	42.5, CH_2	42.0, CH_2	42.6, CH_2	42.4, CH_2	42.6, CH_2	42.1, CH_2	43.0, CH_2
4	17.6, C	34.6, C	34.3, C	34.7, C	34.6, C	34.6, C	34.4, C	34.4, C
5	51.8, CH	54.4, CH	52.8, CH	54.3, CH	54.2, CH	54.2, CH	53.4, CH	56.4, CH
6	22.0, CH_2	20.0, CH_2	131.9, CH	19.2, CH_2	19.1, CH_2	20.1, CH_2	19.5, CH_2	22.0, CH_2
7	28.9, CH_2	34.3, CH_2	123.4, CH	29.9, CH_2	29.4, CH_2	33.6, CH_2	34.0, CH_2	32.8, CH_2
8	136.8, C	141.1, C	129.2, C	136.9, C	133.3, C	138.1, C	138.4, C	39.4, CH
9	136.5, C	139.7, C	135.9, C	139.6, C	138.5, C	136.7, C	138.6, C	56.3, CH
10	38.7, C	41.6, C	42.3, C	41.4, C	41.0, C	41.2, C	41.1, C	39.8, C
11	Nd,[b] C	Nd,[b] C	151.0, C	155.6, C	152.4, C	152.3, C	152.5, C	197.3, C
12	141.0, C	143.5, C	139.5,C	141.2, C	137.5, C	138.8, C	136.0, C	145.7, C
13	138.0, C	133.6, C	133.0, C	138.0, C	134.1, C	129.1, C	127.9, C	135.3, C
14	Nd,[b] C	115.3, C	112.3, C	115.8, C	114.2, C	115.0, C	111.3, C	38.4, CH
15	80.7, CH	60.8, CH	79.5, CH	80.9, CH	79.4, CH	24.4, CH_2	102.2, CH	34.0, CH_2
16	62.4, CH_2	73.3, CH_2	63.6, CH_2	62.6, CH_2	63.4, CH_2	67.5, CH_2	144.1, CH_2	60.6, CH_2
17	Nd,[b] C	166.4, C	172.7, C	172.9, C	172.8, C	167.8, C	163.5, C	12.4, CH_3
18	23.7, CH_3	34.2, CH_3	33.5, CH_3	34.2, CH_3	34.1, CH_3	34.2, CH_3	33.7, CH_3	34.1, CH_3
19	23.1, CH_2	22.7, CH_3	22.9, CH_3	22.6, CH_3	22.4, CH_3	22.7, CH_3	22.2, CH_3	22.3, CH_3
20	16.3, CH_3	19.4, CH_3	17.6, CH_3	19.5, CH_3	19.4, CH_3	19.6, CH_3	19.0, CH_3	15.1, CH_3
OMe	60.8, CH_3	63.2, CH_3		61.1, CH_3				

[a]From inverse-detected HSQC and HMBC experiments. [b]Not detected.

compared to the calculated time-dependent density functional theory (TDDFT) ECD spectrum. The experimental ECD of **1** showed sequential positive Cotton effects (CE) around 290 and 210 nm, which resulted from the n → π^* transition of a carbonyl group and the $\pi \rightarrow \pi^*$ transition of an aromatic part, respectively. Comparison with the calculated ECD spectra for two possible stereoisomers (15*R* and 15*S*) is presented in Figure 2A. The 15*S* stereoisomer showed a complete match with the experimental data, with two positive CEs around 290 and 210 nm, where the other stereoisomer showed a negative CE around 210 nm. Thus, the absolute configuration of **1** was established for the first time as (5*R*,10*S*,15*S*)-swartziarboreol E.

Compound **3** was dereplicated as swartziarboreol A (*m*/*z* 359.1854 $[M + H]^+$, $C_{21}H_{26}O_5$). When compared to **1**, the ^{1}H and ^{13}C NMR chemical shifts at C-15 and C-16 (δ_C 24.0 and 67.3, respectively) were in this case consistent with a dihydropyran unit, while other signals were similar to and in good agreement with those reported for swartziarboreol A.[23] The calculated ECD spectrum for the 5*R*,10*S* stereoisomer showed an excellent fit to the experimental data of **3** (Figure 2B), and its absolute configuration was thus established for the first time as 5*R* and 10*S*.

Compound **4** was dereplicated as swartziarboreol B[23] (Table S1, Supporting Information). NMR analysis was used to confirm the identity of this compound.[23] It displayed a new chromophoric system with charge delocalization causing an absorption at longer wavelength (325 nm) (Figure 2C). In the ECD spectrum, three positive CEs around 280, 245, and 210 nm with one negative CE at 325 nm were observed. These transitions were due to $\pi \rightarrow \pi^*$ transitions of an extended benzo-α-pyrone (coumarin) moiety. As for **1** and **3**, the excellent fit between the experimental and calculated ECD spectra was used to confirm the absolute configuration of **4** as 5*R*,10*S*.

Compound **5** was isolated as an amorphous solid. The HRESIMS showed a $[M - H]^-$ peak at *m*/*z* 357.1716, consistent with an elemental formula of $C_{21}H_{26}O_5$. The ^{1}H and HSQC NMR spectra of **5** were similar to swartziarboreol E (**1**), but showed signals for two instead of three methyl groups, an additional methine at δ_H 0.69, and two upfield protons at δ_H 0.13 and 0.53, characteristic of cyclopropane-ring methylene protons. The presence of a cyclopropane ring was confirmed by the HMBC correlations between CH_3-18 (δ_H 1.10) with the carbons at δ_C 19.5 (C-3), 17.6 (C-4), 51.8 (C-5), and 23.1 (C-

DOI: 10.1021/acs.jnatprod.5b00744
J. Nat. Prod. XXXX, XXX, XXX−XXX

19) (Figure S6, Supporting Information). The relative configuration of ring A and B was deduced by conducting a NOESY experiment. The key NOE correlations from H-5 to H-1ax, H-19″, and H-7ax indicated that they are cofacial with an α-alignment (Figure 3A). On the other hand, dipolar correlations were observed from CH_3-20 to H-6ax and CH_3-18. On the basis of the NMR data and ECD analysis (Figure 2D), the absolute configuration of **5** was determined as 3*S*,4*R*,5*S*,10*S*,15*S*, and it was established as a new diterpene and named simplexene A.

Compound **6** displayed a $[M - H]^-$ peak at *m/z* 359.1863 and a molecular formula of $C_{21}H_{28}O_5$, which did not match any previously isolated compounds from the genus *Swartzia*. The NMR data indicated a similar skeleton to that of swartziarboreol A (**3**),[23] with three methyls and one oxygenated methyl and only one carbonyl signal at δ_C 166.4 at C-17. Moreover, **6** showed an additional signal at δ_H 5.00 integrating for one proton. According to the HSQC spectrum, this proton was attached to an oxygenated carbon at δ_C 60.8, suggesting the presence of a hydroxy group. The position of a hydroxy group at C-15 was supported by COSY correlations between H-15 and H-16 (δ_H 4.47 and 4.34) and by HMBC correlations between H-15 and the quaternary carbons at δ_C 143.5 (C-12), 133.6 (C-13), 115.3 (C-14), and 73.3 (C-16). Comparison between the calculated and experimental ECD spectra obtained indicated a 5*S*,10*S*,15*S* absolute configuration (Figure 2E), and **6** was established as (5*S*,10*S*)-11,15(*S*)-dihydroxy-12-methoxyswartziarboreol G, a new cassane diterpene.

The HRESIMS of **7** exhibited a $[M - H]^-$ peak at *m/z* 343.1544 and a molecular formula of $C_{20}H_{24}O_5$. The 2D NMR data revealed signals for a methine at δ_C 79.5 (C-15), a methylene at δ_C 63.6 (C-16), and an ester at δ_C 172.7 (C-17), similar to those found in swartziarboreol E (**1**). In comparison to **1**, however, the carbonyl at C-3 and the methoxy group at C-12 were missing. The ^{13}C APT spectrum showed signals for two sp^2 methines (δ_C 131.9 and 123.4), suggesting the presence of a double bond (Table 1). The position of the double bond at C-6/C-7 was obtained from the COSY correlations with H-5 at δ_H 2.18 (Figure S15, Supporting Information). The TDDFT-calculated ECD spectrum for 5*S*,10*S*,15*S* showed an excellent fit with the experimental ECD spectrum with three positive and two negative CEs (Figure 2F), whereas the other stereoisomer showed a different pattern. Thus, the absolute configuration of **7** at C-15 was proposed as *S*. This is a new diterpene that was named simplexene B.

The ^1H and ^{13}C NMR spectra of **8** (*m/z* 359.1845 $[M - H]^-$, $C_{21}H_{28}O_5$) were closely related to those of **1**, but a methylene signal (δ_C 42.6), similar to that found in **7**, replaced the carbonyl at C-3 in **1**. As for **7**, the ECD revealed a 5*S*,10*S*,15*S* (Figure 2G) absolute configuration, so **8** was elucidated as a new diterpene named simplexene C.

The ^1H and ^{13}C NMR spectra of **9** were closely related to that of **8**, but with a methoxy group signal missing at C-12. This was also supported by a difference of CH_2 in the molecular formula of **9** ($C_{20}H_{26}O_5$) when compared to **8**. The absence of a methoxy group at C-12 caused a charge delocalization on the chromophore, and a bathochromic shift was observed in the ECD spectrum of **8** when compared to that of **9**. The calculated ECD spectrum for the 5*S*,10*S*,15*R* configuration showed a good fit with the experimental data, with two positive CEs and one negative CE around 205, 260, and 310 nm, respectively, whereas changing the configuration at C-15 to *S* showed an opposite-sign CE at 205 nm (Figure 2H). Thus, the absolute configuration of the new diterpenoid **9**, simplexene D, was established as 5*S*,10*S*,15*R*.

Compound **10** (*m/z* 331.1917 $[M + H]^+$, $C_{20}H_{26}O_4$) exhibited similar characteristic signals for a dihydropyran unit to those present in **3**. The absence of a methoxy group signal at C-12 and a chemical shift of δ_C 138.8 supported the occurrence of a hydroxy group at C-12. The same substitution pattern was observed for the rings, including carbons C-1 to C-10, as for compounds **6**, **7**, and **9**. Accordingly, compound **10** was thus assigned as 11,12-dihydroxy-15,16-dihydroswartziarboreol C. This compound was described before from *S. langsdorffii*, based on only online MS data, with no other supporting spectroscopic data published.[27]

Compound **12** (*m/z* 327.1604 $[M - H]^-$, $C_{20}H_{24}O_4$) presented an additional unsaturation when compared to **10**, with two hydrogens less in its molecular formula. The NMR data were similar to those of **10** with the exception of the presence of two olefinic protons at δ_H 6.76 (1H, d, J = 5.3 Hz, H-15) and 7.25 (1H, d, J = 5.3 Hz, H-16). Therefore, compound **12** was assigned as 11,12-dihydroxy-8,11,13,15-cassatetraen-17,16-olide, thus confirming the dereplication results. As for **10**, the occurrence of **12** was assigned as reported from *S. langsdorffii*, but no spectroscopic data were published.[25] Compound **12** was assigned as 11,12-dihydroxy-swartziarboreol C.

Compounds **11** and **13** were dereplicated as 15,16-dihydroswartziarboreol C[25] and swartziarboreol C,[23] respectively. Their HRESIMS and NMR data as obtained confirmed the structures proposed previously for these compounds. The ECD spectra of the cassane diterpenes **10**–**13** all matched the TDDFT-calculated ECD spectra in terms of the 5*S*,10*S* configuration, which is reported here for the first time for each of these substances (Figure 2).

Compound **14** was isolated as an amorphous solid. Its UV spectrum was different from those of the previously described compounds with a maximum at 278 nm, suggesting a different chromophore. Its $[M + H]^+$ peak at *m/z* 321.2435 indicated $C_{20}H_{32}O_3$ as the molecular formula. The HSQC and HMBC spectra showed 20 carbons, including one carbonyl (δ_C 197.3), two quaternary carbons (δ_C 34.4 and 39.8 for C-4 and C-10, respectively), two quaternary sp^2 carbons (δ_C 135.3 and 145.7 for C-13 and C-12, respectively), four methyls (δ_C 12.4, 15.1, 22.3, and 34.1 for C-17, C-20, C-19, and C-18, respectively), seven methylenes (δ_C 19.5, 22.0, 32.8, 34.0, 41.2, 43.0, and 60.6 for C-2, C-6, C-7, C-15, C-1, C-3, and C-16, respectively), and four methines (δ_C 38.4, 39.4, 56.3, and 56.4 for C-14, C-8, C-9, and C-5, respectively) (Figures S46 and S47, Supporting Information). A comparison with the other isolated diterpenes indicated that the double bond between C-8 and C-9 is replaced by two methines at H-8 and H-9 (δ_H 2.25 and 2.01, respectively), as shown from the HMBC correlations between the methyl CH_3-20 and the methine C-9 and the COSY correlations between H-9 and H-8. A fourth methyl group CH_3-17, δ_H 1.03 (d, J = 6.8 Hz), was positioned at C-14 due to the HMBC correlations with C-9, C-13, and C-14, whereas the carbonyl was placed in C-11 from its correlation with H-9. A primary alcohol group (δ_H 2.26/2.69 for H-15 and 3.72 for H-16) was linked to C-13 as indicated by the correlation from H-15 to C-12, C-13, and C-14. The NOESY correlations from H-9ax to H-1ax and H-5ax, from H-7ax to CH_3-17, and from CH_3-18 to H-6eq indicated all of these protons to be positioned on the same side of the molecule of **14**. For the other side of the molecule, NOESY correlations from CH_3-19 to CH_3-20 and H-

DOI: 10.1021/acs.jnatprod.5b00744
J. Nat. Prod. XXXX, XXX, XXX−XXX

6ax allowed the establishment of the relative configuration of this compound (Figure 3B). The simulated ECD spectrum of the 8*S*,9*S*,14*R* stereoisomer showed two positive CEs and one negative CE around 325, 205, and 295 nm, respectively, which was in good agreement with the experimental ECD spectrum, whereas the other stereoisomers showed different patterns. On the basis of these observations, the absolute configuration of **14**, simplexene E, was determined as 5*S*,8*S*,9*S*,10*S*,14*R*, with the structure as shown.

The antifungal activities of all isolated compounds were determined on both wild-type and hypersusceptible strains of *C. albicans* in both bioautography and dilution assays for a comprehensive evaluation of their minimal inhibitory quantity (MIQ) and minimal inhibitory concentration (MIC) values, respectively (Table 2). The MIQ values against the mutant strain (DSY2621) were consistent with the HPLC microfractionation results. Assessment on the same amount of each isolated compound revealed that only **4**, **6**, **8**, **9**, and **10** gave a MIQ value between 5 and 20 μg against the mutant strain. All other compounds were found inactive at the higher dose tested of 50 μg. The antifungal agents **4** and **6** that were found against the hypersusceptible strain by HPLC activity-based profiling were thus detected at-line, since according to the ELSD trace, they were present in only minute amounts in the extracts (Figure 1). As expected, and since the hypersusceptible strain was used only for the detection of minor compounds, the MIQ values against the wild-type strain were in general higher, and only compound **6** had a significant activity (MIQ of 2 μg) and could be considered as a lead compound of interest.[28]

Table 2. Bioautography, Broth Dilution Assay, and Biofilm Evaluation of the *S. simplex* Root Extract and Isolated and Reference Compound

	bioautography assay MIQ		dilution assay MIC	mature biofilm MIC
extract/compound	*C. albicans* (DSY2621)[a]	*C. albicans* (CAF2-1)[a]	*C. albicans* (CAF2-1)[b]	*C. albicans* (CAF2-1)[b]
crude extract	20 μg	[d]	[d]	[d]
1	[d]	[d]	[d]	[d]
2	[d]	[d]	[d]	[d]
3	[d]	[d]	[d]	[d]
4	10 μg	[d]	[d]	[d]
5	ND[e]	ND[e]	[d]	50 μg/mL
6	5 μg	2 μg	32 μg/mL	50 μg/mL
7	[d]	[d]	[d]	50 μg/mL
8	20 μg	[d]	[d]	[d]
9	8 μg	[d]	32 μg/mL	25 μg/mL
10	8 μg	[d]	[d]	50 μg/mL
11	[d]	[d]	[d]	[d]
12	ND[e]	ND[e]	[d]	50 μg/mL
13	[d]	[d]	[d]	[d]
14	<20 μg	ND[e]	[d]	[d]
miconazole[c]	0.0006 μg	0.005 μg	0.0156 μg/mL	ND[e]

[a]Minimum amount required for antifungal activity on a TLC plate. [b]Minimum inhibitory concentration. [c]Reference compound. [d]Inactive: MIQ > 50 μg; MIC > 32 μg/mL; biofilm > 50 μg/mL. [e]ND: not determined.

Broth dilution methods are the reference methods for antifungal susceptibility testing and are used mainly to evaluate the activity of new antifungal agents.[29] The MICs of the compounds were determined according to the EUCAST method. Compounds **6** and **9** exhibited notable activity, both with a MIC of 32 μg/mL against the *C. albicans* wild-type strain (Table 2).

As most *C. albicans* cells do not exist as free-living organisms but rather as groups of cells within an organized biofilm, and because biofilms display different properties that increase their resistance to antifungal drugs,[30] the activity of the compounds against wild-type CAF2-1 biofilms was assessed. Several parameters of this method, such as the medium, the incubation temperature, and the inoculum concentration, differ from those of the EUCAST method to allow the formation of *C. albicans* biofilms. Compounds **5**, **6**, **7**, **10**, and **12** inhibited mature biofilm growth, all with MIC values of 50 μg/mL, and **9** exhibited a MIC value of 25 μg/mL.

Since **9** (simplexene D) exhibited the lowest MIC against both planktonic and biofilm forms of the *C. albicans* wild-type strain, the cytological effects of this antifungal agent were assessed by transmission electron microscopy (TEM). Potential alterations of **9** on the ultrastructure of *C. albicans* wild-type CAF2-1 was evaluated on thin sections by TEM. The yeast was grown on YNB medium at pH 4.6 and treated with compound **9** at the MIC concentration. In comparison to the positive and negative controls, which exhibited the same growth and cytological morphology, CAF2-1 cells treated with **9** showed very important alterations and breakage zones of the plasma membrane (Figure 4). An evident disorganization of the cytoplasmic content was observed, where neither mitochondria nor Golgi apparatus or ribosomes were visible. Retraction of the cytoplasm was noticed, as well as disorganization and disruption of the nuclear membrane (Figure 4D). In some cases, the intact part of the cell was still able to initiate budding. In the altered parts, budding did not seem to occur, and the wall itself was altered (Figure 4D). Contrary to what was previously shown after treatment with miconazole,[18] a reference drug, no accumulation of lipid-like bodies was observed in

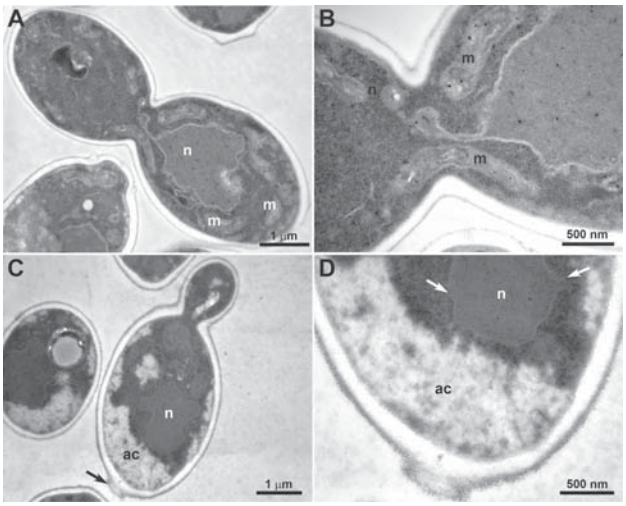

Figure 4. Ultrastructure of *C. albicans* CAF2-1 as a control using DMSO alone at 18 h or after 18 h treatment with compound **9** observed by transmission electron microscopy. (A) Control with DMSO treatment. The black arrow shows alteration of the cell wall. (B) Details of A. (C) After treatment with compound **9** at 16 μg/mL. (D) Details of C. White arrows show zones of alteration of the nuclear membrane. ac: altered part of the cytoplasmic content; m: mitochondrion; n: nucleus.

DOI: 10.1021/acs.jnatprod.5b00744
J. Nat. Prod. XXXX, XXX, XXX−XXX

vacuoles, neither dark material in the parietal zone nor highly contrasted membranes. These results suggested that **9** exerts different cytological effects on *C. albicans* and should further be investigated from a mechanistic point of view.

EXPERIMENTAL SECTION

General Experimental Procedures. The optical rotations were measured in methanolic solutions on a JASCO polarimeter in a 1 cm tube. The ECD spectra were recorded in MeOH with a Chirascan CD spectrometer. The UV spectra were measured on a HACH UV−vis DR/4000 instrument. ^{1}H and ^{13}C NMR data were recorded on an Agilent Varian Inova 500 MHz NMR spectrometer (Palo Alto, CA, USA) (499.88 and 125.71 MHz, respectively). Chemical shifts are reported in parts per million (δ) using the residual MeOD signal (δ_H 3.31; δ_C 49.0) as internal standards for ^{1}H and ^{13}C NMR, respectively, and coupling constants (J) are reported in Hz. Complete assignments were obtained using 2D experiments including COSY, edited-HSQC, HMBC, and NOESY. HRESIMS data were obtained on a Micromass-LCT Premier time of flight (TOF) mass spectrometer (Waters, Milford, MA, USA) with an electrospray interface and coupled with an Acquity UPLC system (Waters). HPLC-PDA-ELSD data were obtained with an Agilent 1100 series system (Santa Clara, CA, USA) consisting of an autosampler, high-pressure mixing pump, and PDA detector connected to an ELSD (Sedex 85, Sedere Omnilab). MPLC separation was performed using a Buchi 681 pump equipped with a Knauer UV detector and a 460 × 70 mm i.d. column (Büchi, Flawil, Switzerland) loaded with Zeoprep C_{18} 15−25 μm as the stationary phase (Zeochem, Uetikon am See, Switzerland). Semi-preparative HPLC was carried out with a Shimadzu LC-8A pump (Columbia, MD, USA) equipped with a UV detector. Micro-fractionation was performed on a modular HPLC system, comprising a Varian 9012 pump, a Valco injection valve with a loop of 200 μL, a Knauer UV detector (Berlin, Germany), and a recorder (LKB rec 1; Sollentuna, Sweden). Conformational analysis of the isolated compounds was performed with Schrödinger MacroModel 9.1 (Schrödinger, LLC, New York, USA) employing the OPLS2005 (optimized potential for liquid simulations) force field in H_2O.

Plant Material. The root bark of the roots of *Swartzia simplex* was collected in Coclé, Barrigón, El Copé, Panama (November 1996). The plant was identified by Dr. Alex Espinosa of CIFLORPAN, University of Panama. A voucher specimen (no. 7094) has been deposited at the National Herbarium of Panama, Panama City.

Extraction and Isolation. The air-dried plant material was pulverized in a Wiley mill, providing 615 g of a fine powder, and extracted at room temperature successively with hexane, CH_2Cl_2, methanol (MeOH), and water (H_2O) to give 3.9, 20.6, 44.6, and 11.3 g, respectively. The extracts were concentrated under pressure and later lyophilized. In this investigation only the CH_2Cl_2 extract was investigated. The crude CH_2Cl_2 extract (5.5 g) was first fractionated using reversed-phase MPLC with a 460 × 70 mm i.d. column (Büchi, Flawil, Switzerland), loaded with Zeoprep C_{18} 15−25 μm as the stationary phase (Zeochem, Uetikon am See, Switzerland), with a linear gradient of MeOH and H_2O from 5% to 100% MeOH with 0.1% formic acid, and yielded 118 fractions. The separation conditions were optimized at the analytical HPLC level with the same stationary phase chemistry and geometrically transferred by gradient transfer.[26] Fractions F35, F51, F58, and F72 consisted of pure **1** (6.2 mg), **3** (47.5 mg), **4** (15.4 mg), and **7** (27.8 mg), respectively. The final purification was performed using different selectivity by semipreparative normal-phase HPLC on a Cosmosil column (250 × 10 mm i.d., 5 μm, Phenomenex, Torrance, CA, USA) with EtOAc−hexane as eluents. Fractions 46 and 47 (14.2 mg) yielded **2** (1.6 mg) and **3** (10 mg) (isocratic conditions with EtOAc 50%, flow rate 4.7 mL/min, UV 254 nm); fractions F67 and 68 (14.6 mg) led to the isolation of **5** (0.2 mg) and **6** (0.5 mg) (isocratic conditions with EtOAc 40%). The group fractions 74, 75, and 76 (14 mg) afforded **8** (0.4 mg) and **9** (0.4 mg) (gradient conditions 20% EtOAc during 22 min, from 22% to 55% in 12 min, from 55% to 70% in 40 min), and fractions F82 and 83 (36.6 mg) afforded **8** (7.8 mg) and **10** (6.9 mg) (EtOAc 22% isocratic conditions). The final purification of some fractions was performed by semipreparative reversed-phase HPLC using an X-Bridge C_{18} column (150 × 10 mm, i.d. 5 μm; Waters) using MeOH−H_2O as eluents for isocratic elution. Fractions F94−97 (40 mg) yielded **11** (12.5 mg), **13** (0.7 mg), and **14** (0.8 mg) (70% MeOH). MeCN was used instead of MeOH in the case of fraction F84 (16.6 mg), which yielded **12** (1.5 mg) (MeCN 52% isocratic condition).

*Simplexene A (**5**):* amorphous solid; $[\alpha]^{25}_D$ −5.5 (*c* 0.1, MeOH); UV λ_{max} (MeCN) (log ε) 219 (3.61), 263 (2.40) nm; ECD (MeOH, *c* 0.6 mM, 0.1 cm) $[\theta]_{289}$ −1606, $[\theta]_{267}$ 3968, $[\theta]_{241}$ −3322, $[\theta]_{209}$ 26836; ^{1}H NMR (MeOD, 500 MHz) δ 0.13 (1H, dd, *J* = 5.7, 4.1 Hz, H-19″), 0.53 (1H, dd, *J* = 9.2, 4.0 Hz, H-19′), 0.69 (1H, ddd, *J* = 9.2, 7.2, 5.7 Hz, H-3), 0.81 (1H, td, *J* = 13.0, 6.4 Hz, H-1ax), 1.10 (3H, s, CH_3-18), 1.37 (3H, s, CH_3-20), 1.44 (1H, d, *J* = 13.0 Hz, H-5ax), 1.63 (1H, qd, *J* = 12.9, 5.0 Hz, H-6ax), 1.78 (1H, dd, *J* = 14.1, 6.4 Hz, H-2eq), 2.07 (1H, dd, *J* = 13.1, 6.3 Hz, H-6eq), 2.20 (1H, tt, *J* = 14.1, 7.2 Hz, H-2ax), 2.77 (1H, ddd, *J* = 18.6, 12.5, 6.4 Hz, H-7ax), 3.05 (1H, dd, *J* = 13.3, 7.3 Hz, H-1eq), 3.51 (1H, ddd, *J* = 18.2, 5.0, 1.5 Hz, H-7eq), 3.79 (3H, s, OCH_3), 3.81 (1H, dd, *J* = 12.5, 4.8 Hz, H-16″), 4.16 (1H, dd, *J* = 12.5, 2.5 Hz, H-16′), 5.57 (1H, dd, *J* = 4.9, 2.5 Hz, H-15); ^{13}C NMR, see Table 1; ESIMS *m*/*z* 357.1716 [M − H]$^-$, calcd for $C_{21}H_{25}O_5$, 357.1702.

*(5S,10S)-11,15(R)-Dihydroxy,12-methoxyswartziarboreol G (**6**):* amorphous solid; $[\alpha]^{25}_D$ +250 (*c* 0.02, MeCN); UV λ_{max} (MeCN) (log ε) 220 (3.91), 266 (3.48), 300 (sh) nm; ECD (MeOH, *c* 0.5 mM, 0.1 cm) $[\theta]_{321}$ −1386, $[\theta]_{268}$ 11457, $[\theta]_{218}$ 4936; ^{1}H NMR (MeOD, 500 MHz) δ 0.96 (3H, s, CH_3-19), 0.99 (3H, s, CH_3-18), 1.13 (1H, td, *J* = 13.0, 3.5 Hz, H-1ax), 1.26 (1H, d, *J* = 12.6 Hz, H-5), 1.26 (1H, td, *J* = 13.0, 3.5 Hz, H-3ax), 1.37 (3H, s, CH_3-20), 1.44 (1H, qd, *J* = 12.6, 4.8 Hz, H-6ax), 1.49 (1H, dt, *J* = 13.0, 3.5 Hz, H-3eq), 1.53 (1H, dp, *J* = 13.0, 3.5 Hz, H-2eq), 1.78 (1H, qt, *J* = 13.0, 3.5 Hz, H-2ax), 1.88 (1H, ddd, *J* = 12.6, 6.5, 1.6 Hz, H-6eq), 2.97 (1H, ddd, *J* = 18.4, 4.8, 1.6 Hz, H-7eq), 3.26 (1H, ddd, *J* = 18.4, 12.7, 6.5 Hz, H-7ax), 3.34 (1H, m, H-1eq), 3.84 (3H, s, OCH_3), 4.34 (1H, dd, *J* = 12.0, 1.7 Hz, H-16″), 4.47 (1H, dd, *J* = 12.0, 1.7 Hz, H-16′), 5.00 (1H, t, *J* = 1.7 Hz, H-15); ^{13}C NMR, see Table 1; ESIMS *m*/*z* 359.1863 [M − H]$^-$, calcd for $C_{21}H_{27}O_5$, 359.1858.

*Simplexene B (**7**):* amorphous solid; $[\alpha]^{25}_D$ +185 (*c* 0.02, MeCN); UV λ_{max} (MeCN) (log ε) 213 (4.28), 263 (4.05), 328 (3.63) nm; ECD (MeOH, *c* 0.4 mM, 0.1 cm) $[\theta]_{306}$ −3171, $[\theta]_{270}$ 2972, $[\theta]_{250}$ −2209, $[\theta]_{232}$ 9358, $[\theta]_{206}$ 24203; ^{1}H NMR (MeOD, 500 MHz) δ 1.00 (3H, s, CH_3-18), 1.07 (3H, s, CH_3-19), 1.13 (3H, s, CH_3-20), 1.29 (1H, t, *J* = 13.0 Hz, H-3ax), 1.50 (1H, d, *J* = 13.0 Hz, H-3eq), 1.61 (1H, dp, *J* = 13.0, 3.5 Hz, H-2eq), 1.71 (1H, t, *J* = 13.0 Hz, H-1ax), 1.76 (1H, qt, *J* = 13.0, 3.5 Hz, H-2ax), 2.18 (1H, t, *J* = 3.0 Hz, H-5), 3.22 (1H, d, *J* = 13.3 Hz, H-1eq), 3.83 (1H, dd, *J* = 10.9, 6.5 Hz, H-16″), 4.06 (1H, dd, *J* = 10.9, 5.0 Hz, H-16′), 5.42 (1H, dd, *J* = 6.5, 5.0 Hz, H-15), 6.11 (1H, dd, *J* = 9.8, 3.0 Hz, H-6), 7.44 (1H, dd, *J* = 9.8, 3.0 Hz, H-7); ^{13}C NMR, see Table 1; ESIMS *m*/*z* 343.1544 [M − H]$^-$, calcd for $C_{20}H_{23}O_5$, 343.1545.

*Simplexene C (**8**):* amorphous solid; $[\alpha]^{25}_D$ +82 (*c* 0.1, MeOH); UV λ_{max} (MeCN) (log ε) 2200 (3.96), 250 (sh, 3.39), 266 (3.54), nm; ECD (MeOH, *c* 0.6 mM, 0.1 cm) $[\theta]_{208}$ 27410, $[\theta]_{243}$ −4408; ^{1}H NMR (MeOD, 500 MHz) δ 0.96 (3H, s, CH_3-19), 0.99 (3H, s, CH_3-18), 1.15 (1H, td, *J* = 13.0, 3.4 Hz, H-1ax), 1.27 (1H, td, *J* = 13.8, 3.4 Hz, H-3ax), 1.28 (1H, d, *J* = 10.6 Hz, H-5), 1.36 (3H, s, CH_3-20), 1.48 (1H, dt, *J* = 13.8, 3.4 Hz, H-3eq), 1.52 (1H, dp, *J* = 13.0, 3.4 Hz, H-2eq), 1.53 (1H, qd, *J* = 13.0, 5.4 Hz, H-6ax), 1.78 (1H, qt, *J* = 13.0, 3.4 Hz, H-2ax), 1.92 (1H, dd, *J* = 13.1, 6.9 Hz, H-6eq), 2.86 (1H, ddd, *J* = 18.8, 12.6, 6.9 Hz, H-7ax), 3.36 (1H, dt, *J* = 13.0, 3.4 Hz, H-1eq), 3.41 (1H, ddd, *J* = 18.8, 5.4, 1.4 Hz, H-7eq), 3.80 (3H, s, OCH_3), 3.81 (1H, dd, *J* = 12.6, 4.9 Hz, H-16″), 4.16 (1H, dd, *J* = 12.6, 2.4 Hz, H-16′), 5.57 (1H, dd, *J* = 4.9, 2.4 Hz, H-15); ^{13}C NMR, see Table 1; ESITOFMS *m*/*z* 359.1845 [M − H]$^-$, calcd for $C_{21}H_{27}O_5$, 359.1858.

*Simplexene D (**9**):* amorphous solid; $[\alpha]^{25}_D$ +245 (*c* 0.02, MeCN); UV λ_{max} (MeCN) (log ε) 218 (4.49), 268 (4.04), 300 (3.63) nm; ECD (MeOH, *c* 0.4 mM, 0.1 cm) $[\theta]_{297}$ −7251, $[\theta]_{259}$ 18 224, $[\theta]_{209}$ 3978; ^{1}H NMR (MeOD, 500 MHz) δ 0.96 (3H, s, CH_3-19), 0.98 (3H, s, CH_3-18), 1.14 (1H, td, *J* = 13.0, 3.0 Hz, H-1ax), 1.26 (1H, td, *J* = 13.0, 3.0 Hz, H-3ax), 1.28 (1H, d, *J* = 13.0 Hz, H-5), 1.37 (3H, s, CH_3-20),

DOI: 10.1021/acs.jnatprod.5b00744
J. Nat. Prod. XXXX, XXX, XXX−XXX

1.48 (1H, dt, J = 13.0, 3.0 Hz, H-3eq), 1.51 (1H, dp, J = 13.0, 3.0 Hz, H-2eq), 1.52 (1H, qd, J = 13.0, 5.4 Hz, H-6ax), 1.77 (1H, qt, J = 13.0, 3.0 Hz, H-2ax), 1.90 (1H, dd, J = 13.0, 6.8 Hz, H-6eq), 2.83 (1H, ddd, J = 18.6, 12.6, 6.8 Hz, H-7ax), 3.36 (1H, dt, J = 13.0, 3.0 Hz, H-1eq), 3.37 (1H, dd, J = 18.6, 5.4 Hz, H-7eq), 3.83 (1H, dd, J = 11.1, 5.5 Hz, H-16″), 3.96 (1H, dd, J = 11.1, 5.5 Hz, H-16′), 5.41 (1H, t, J = 5.5 Hz, H-15); ^{13}C NMR, see Table 1; ESIMS m/z 345.1695 $[M - H]^-$, calcd for $C_{20}H_{25}O_5$, 345.1702.

*11,12-Dihydroxy-15,16-dihydroswartziarboreol C (**10**):* amorphous solid; $[\alpha]^{25}_D$ +139.2 (c 0.1, MeOH); UV λ_{max} (MeCN) (log ε) 217 (4.33), 270 (3.88), 301 (3.48) nm; ECD (MeOH, c 0.3 mM, 0.1 cm) $[\theta]_{276}$ 6722, $[\theta]_{236}$ 14 152, $[\theta]_{207}$ 21 087; ^{1}H NMR (MeOD, 500 MHz) δ 0.95 (3H, s, CH_3-19), 0.98 (3H, s, CH_3-18), 1.11 (1H, td, J = 13.5, 4.0 Hz, H-1′), 1.24 (1H, d, J = 12.4 Hz, H-5), 1.25 (1H, td, J = 13.5, 4.0 Hz, H-3′), 1.37 (3H, s, CH_3-20), 1.45 (1H, qd, J = 12.9, 12.4, 12.4, 5.4 Hz, H-6′), 1.47 (1H, dt, J = 13.5, 4.0 Hz, H-3″), 1.51 (1H, dp, J = 13.5, 4.0 Hz, H-2″), 1.77 (1H, qt, J = 13.5, 4.0 Hz, H-2′), 1.85 (1H, ddd, J = 12.9, 6.6, 1.9 Hz, H-6″), 2.85 (1H, ddd, J = 16.3, 10.7, 4.7 Hz, H-15′), 2.97 (1H, dt, J = 16.3, 4.7, 3.5 Hz, H-15″), 3.07 (1H, ddd, J = 18.4, 12.4, 6.6 Hz, H-7′), 3.16 (1H, ddd, J = 18.4, 5.4, 1.9 Hz, H-7″), 3.34 (1H, dt, J = 13.5, 4.0 Hz, H-1″), 4.25 (1H, td, J = 10.7, 3.5 Hz, H-16′), 4.38 (1H, dt, J = 10.7, 4.7, 3.5 Hz, H-16″); ^{13}C NMR, see Table 1; ESIMS m/z 331.1917 $[M + H]^+$, calcd for $C_{20}H_{27}O_4$, 331.1909.

*15,16-Dihydroswartziarboreol C (**11**):* amorphous solid; $[\alpha]^{25}_D$ +235 (c 0.02, MeCN); UV λ_{max} (MeCN) (log ε) 220 (4.40), 267 (4.03), 340 (3.1) nm; ECD (MeOH, c 0.5 mM, 0.1 cm) $[\theta]_{277}$ 7469, $[\theta]_{213}$ 24829; ESITOFMS m/z 343.1882 $[M - H]^-$, calcd for $C_{21}H_{27}O_4$, 343.1909.

*11,12-Dihydroxy-8,11,13,15-cassatetraen-17,16-olide named 11,12-Dihydroxyswartziarboreol C (**12**):* amorphous solid; $[\alpha]^{25}_D$ +150 (c 0.02, MeCN); UV λ_{max} (MeCN) (log ε) 267 (4.2), 299 (3.8), 345.5 (2.6) nm; ECD (MeOH, c 0.8 mM, 0.1 cm) $[\theta]_{327}$ −1032, $[\theta]_{213}$ 5379; 216.68 (3.98), 247.88 (4.06), 320.73 (3.28) nm; ^{1}H NMR (MeOD, 500 MHz) δ 0.95 (3H, s, CH_3-19), 0.98 (3H, s, CH_3-18), 1.08 (1H, td, J = 12.5, 4.0 Hz, H-1ax), 1.23 (1H, d, J = 12.0 Hz, H-5), 1.24 (1H, td, J = 12.5, 4.0 Hz, H-3ax), 1.41 (3H, s, CH_3-20), 1.46 (1H, dt, J = 12.5, 4.0 Hz, H-3eq), 1.49 (1H, q, J = 12.9, 12.4, 12.0 Hz, H-6ax), 1.50 (1H, dp, J = 12.5, 4.0 Hz, H-2eq), 1.76 (1H, qt, J = 12.5, 4.0 Hz, H-2ax), 1.91 (1H, dd, J = 12.9, 6.8 Hz, H-6eq), 3.15 (1H, ddd, J = 19.2, 12.4, 7.1 Hz, H-7′), 3.33 (1H, dt, J = 12.5, 4.0 Hz, H-1eq), 3.39 (1H, dd, J = 19.2, 5.5 Hz, H-7″), 6.76 (1H, d, J = 5.3 Hz, H-15), 7.25 (1H, d, J = 5.3 Hz, H-16); ^{13}C NMR, see Table 1; ESIMS m/z 327.1604 $[M - H]^-$, calcd for $C_{20}H_{23}O_4$, 327.1596; m/z 655.3289 $[2M - H]^-$, calcd for $C_{40}H_{47}O_8$, 655.3271.

*Simplexene E (**14**):* amorphous solid; $[\alpha]^{25}_D$ +248 (c 0.02, MeCN); UV λ_{max} (MeCN) (log ε) 277.8 (4.13) nm; ECD (MeOH, c 0.6 mM, 0.1 cm) $[\theta]_{326}$ 7068, $[\theta]_{291}$ −1296, $[\theta]_{268}$ 1806, $[\theta]_{206}$ 10 789; ^{1}H NMR (MeOD, 500 MHz) δ 0.86 (3H, s, CH_3-19), 0.89 (3H, s, CH_3-18), 0.92 (1H, dd, J = 12.1, 2.2 Hz, H-5), 0.96 (3H, s, CH_3-20), 1.03 (3H, d, J = 6.8 Hz, CH_3-17), 1.13 (1H, td, J = 13.5, 4.0 Hz, H-1ax), 1.24 (1H, td, J = 13.5, 4.0 Hz, H-3ax), 1.36 (1H, qd, J = 12.2, 3.0 Hz, H-6ax), 1.40 (1H, dt, J = 13.5, 4.0 Hz, H-3eq), 1.42 (1H, dp, J = 13.5, 4.0 Hz, H-2eq), 1.48 (1H, qd, J = 12.2, 3.0 Hz, H-7ax), 1.63 (1H, qt, J = 13.5, 4.0 Hz, H-2ax), 1.65 (1H, dq, J = 12.3, 3.0 Hz, H-7eq), 1.69 (1H, dq, J = 12.2, 3.0 Hz, H-6eq), 2.01 (1H, d, J = 13.0 Hz, H-9), 2.25 (1H, m, H-8), 2.26 (1H, m, H-15″), 2.27 (1H, m, H-14), 2.69 (1H, dt, J = 13.0, 7.1 Hz, H-15′), 3.03 (1H, dt, J = 13.8, 4.0 Hz, H-1eq), 3.72 (2H, t, J = 7.1 Hz, CH_2-16); ^{13}C NMR, see Table 1; ESIMS m/z 321.2435 $[M + H]^+$, calcd for $C_{20}H_{33}O_3$, 321.243.

Absolute Conformation by Electronic Circular Dichroism. Conformational analysis of the isolated compounds was performed with Schrödinger MacroModel 9.1 (Schrödinger LLC, New Yor, USAk) employing the OPLS2005 force field in H_2O. Conformers within a 2 kcal/mol energy window from the global minimum were selected for geometrical optimization and energy calculation applying DFT with Becke's nonlocal three-parameter exchange and correlation functional and the Lee−Yang−Parr correlation functional level (B3LYP) using the 6-31/G** basis set in the gas phase with the Gaussian 09 program.[31] Vibrational analysis was done at the same level to confirm minima. TD-DFT/B3LYP/6-31G** was conducted in MeOH using the SCRF method, with the CPCM model. ECD curves were constructed on the basis of rotatory strength dipole velocity (R_{vel}), and dipole lengths (R_{len}) were calculated with a half-band of 0.25 eV using SpecDis v1.61.[32]

HPTLC Analysis. HPTLC analysis was performed with an automatic TLC sampler (4) and an automatic developing chamber (ADC 2) (Camag, Muttenz, Switzerland). The plant extract (200 μg) was deposited onto the HPTLC plate (10 × 10 cm, silica gel 60, Merck, Darmstadt, Germany). The CH_2Cl_2 extract was eluted with petroleum ether−ethyl acetate (EtOAc) (50:50). The TLC profiles were revealed by UV detection at 254 and 366 nm with a TLC visualizer (CAMAG), and images were obtained with vision CATS1.4 software. HPTLC analysis was performed in duplicate for the bioautography and for the chemical detection with specific reagents.

Dereplication by UHPLC-HRESIMS/MS Analysis. Chromatographic separation was performed on a Thermo Dionex Ultimate 3000 UHPLC system interfaced to a Q Exactive Plus mass spectrometer (Thermo Scientific, Bremen, Germany), using a heated electrospray ionization (HESI-II) source. The UHPLC conditions were as follows: column, Hypersil gold, 100 × 2.1 mm i.d., 1.9 μm particle size (Thermo Fisher Scientific, Bellefonte, PA, USA); 1 μL of the crude extract at 10 mg/mL was injected. The gradient was performed at a flow rate of 0.6 mL/min with the following solvent system: A = 0.1% formic acid−H_2O, B = 0.1% formic acid−acetonitrile (MeCN); gradient linear: 0% B to 99% of B from 0 to 20 min. The full-scan MS analyses were performed in the positive ionization and negative ionization modes with a mass range of 150−1300 at a resolution of 70 000 full widths at half-maximum (fwhm) (at m/z 200). The ion injection time used was 200 ms. In PI mode, the diisooctyl phthalate ($C_{24}H_{38}O_4$) quasimolecular ion (m/z 391.28429) was used as internal lock mass. The optimized HESI-II parameters were the following: source voltage, 4.0 kV (pos), 2.5 kV (neg); sheath gas flow rate (N_2), 50 units; auxiliary gas flow rate, 12 units; spare gas flow rate, 2.5; capillary temperature, 266.25 °C (pos), 256.25 °C (neg); S-Lens RF level, 50. The mass analyzer was calibrated according to the manufacturer's directions using a mixture of caffeine, methionine−arginine−phenylalanine−alanine-acetate, sodium dodecyl sulfate, sodium taurocholate, and Ultramark 1621 in a MeCN−MeOH−H_2O solution containing 1% acetic acid by direct injection. ThermoRAW data were converted to mzXML using ProteoWizard,[33] an open source software for rapid proteomics tools development. Data treatment and dereplication processes were performed using mzMine 2.10,[34] a modular framework for processing, visualizing, and analyzing mass spectrometry-based molecular profile data.[33] The *Dictionary of Natural Products* was used as a database for the dereplication (http://dnp.chemnetbase.com/).[21]

HPLC-PDA-ELSD Analysis. HPLC-PDA-ELSD data were obtained using an X-Bridge C_{18} column (5 μm, 250 × 4.6 mm i.d.; Waters), solvent system, A = 0.1% formic acid−H_2O, B = 0.1% formic acid−MeOH; gradient mode, 45% to 79% B from 0 to 30 min, held constant at 79% B from 30 to 50 min, from 79% to 100% B in 10 min and held constant at 100% during 10 min; flow rate, 1 mL/min; injection volume, 10 μL; sample concentration, 10 mg/mL in MeOH. The UV traces were recorded at 210 and 254 nm, and UV spectra (PDA) were recorded between 190 and 600 nm (2 nm steps).

HPLC Microfractionation for Antifungal Bioactivity Profiling. A 200 μL aliquot of the CH_2Cl_2 extract of *S. simplex* (25 mg) was injected in an Armen modular spot prep II (Saint-Avé, France) preparative instrument fitted with an X-Bridge C_{18} column (250 × 10 mm i.d.; 5 μm, Waters). The extract was eluted with the specific gradient used for HPLC-PDA-ELSD analysis at a flow rate of 1 mL/min with the following solvent system: A = H_2O; B = MeOH. Detection was performed at 254 nm. The fractions were collected in 50 glass tubes and evaporated to dryness using a SpeedVac (HT-4X Genevac, Stone Ridge, NY, USA). The content of each tube was suspended in 40 μL of MeOH and deposed on the TLC plate of silica gel GF 254-coated A1 sheets (Merck, Darmstadt, Germany) for the biological assay.

DOI: 10.1021/acs.jnatprod.5b00744
J. Nat. Prod. XXXX, XXX, XXX−XXX

Yeast Strains. *Candida albicans* DSY2621 and parent wild-type CAF2-1 (*ura3*Δ::*imm434*/*URA3*) were obtained from Prof. Dominique Sanglard (Institute of Microbiology, University of Lausanne and University Hospital Center). The *C. albicans* hypersusceptible strain DSY2621 was constructed by targeted deletions of genes encoding membrane efflux transporters (*cdr1*Δ::*hisG*/*cdr1*Δ::*hisG*, *cdr2*Δ::*hisG*/*cdr2*Δ::*hisG*, *flu1*Δ::*hisG*/*flu1*Δ::*hisG*, *mdr1*Δ::*hisG*/*mdr1*Δ::*hisG*) and calcineurin subunit A (*cmp1*Δ::*hisG*/*cmp1*Δ::*hisG-URA3-hisG*).[35] The yeast strains were maintained on Sabouraud agar (peptone from meat, 5.0 g/L; peptone from casein, 5.0 g/L; D-(+)-glucose, 40.0 g/L; agar−agar, 15.0 g/L; Merck) Petri dishes.

Bioautography. The assay used was an optimized version of a method published by Rahalison et al.[36] Briefly, the *C. albicans* strains were cultivated overnight at 36 °C in Sabouraud broth medium. A dilution was made in order to obtain an inoculum of 10^5 cells/mL (an optical density (OD) equal to 1 at 630 nm corresponding to approximately 10^7 cells/mL) in malt agar (malt extract, 30.0 g/L; peptone from soymeal, 3.0 g/L; agar−agar, 15.0 g/L; Merck). The molten medium was maintained in a water bath at 45 °C. The OD at 630 nm of the *C. albicans* culture was measured with a UV/vis spectrophotometer (Synergy H1, Biotek, equipped with the software Gen 5.2 software). Approximately 20 mL of the inoculum (either DSY2621 or CAF2-1) was distributed rapidly over the HPTLC plate with a sterile pipet. After solidification of the medium, the plates were incubated overnight at 36 °C in polyethylene boxes lined with moist chromatography paper. The bioautograms were sprayed with an aqueous solution (2.5 mg/mL) of thiazolyl blue (methyl thiazolyl tetrazolium chloride; MTT; Fluka) and incubated for 6 h at 36 °C. Clear inhibition zones were observed against a purple background. To calculate the MIQ, 10 μL aliquots of different concentrations (from 0.01 to 10 mg/mL in MeOH) of the pure compounds were spotted manually on the HPTLC plate as well as 10 μL of only MeOH. Then, the HPTLC plate without elution was submitted to the same procedure. The MIQ was defined as the test compound quantity at which inhibition was observed.

Antifungal Susceptibility Testing. Antifungal susceptibility testing on planktonic cells was carried out on the basis of EUCAST protocols with slight modifications.[37] Briefly, *C. albicans* strains were cultivated overnight at 30 °C under constant agitation in yeast extract peptone dextrose (YEPD). Cultures were diluted to a density of (0.5−2) × 10^5 cells per mL in Roswell Park Memorial Institute medium (RPMI) 1640 medium (Sigma) with L-glutamine, without bicarbonate, and with phenol red as the pH indicator. RPMI 1640 medium was buffered to pH 7 with 0.165 M morpholinepropanesulfonic acid and was supplemented with glucose to a final concentration (wt/vol) of 2% and with 1% dimethyl sulfoxide (DMSO). Compounds were dissolved in DMSO to 1 mg/mL as final concentration. First, 50 μL of RPMI was distributed on each well of the 96-well plate. Twofold serial dilutions were prepared from 32 to 0.0162 μg/mL. Since the yeast inoculum was fixed at a volume of 150 μL with a density of 2 × 10^5 cells/mL, 50 μL of an 8-fold concentrated compound stock was first dispensed to the well corresponding to the highest drug concentration. Twofold dilutions were next performed by serially transferring half volumes of each well up to the last well of the microplate row. Finally, 150 μL of the yeast inoculum was added to each well. Drug-free cultures and sterility controls were included in each 96-well plate. Plates were incubated at 35 °C for 24 h, and then MICs were read with a spectrophotometer plate reader set at 450 nm. The MIC was defined as the drug concentration at which the optical density was equal or decreased more than 50% from that of the drug-free culture.

Antifungal susceptibility assays on biofilms were conducted according to a published protocol.[38] Briefly, an aliquot of a 100 μL solution (1 × 10^6 cells/mL density) per well prepared in the RPMI medium 0.2% glucose (pH 7) was deposited in a 96-well plate and incubated at 37 °C for 48 h to allow biofilm formation. Wells were then washed twice with phosphate-buffered saline (PBS). Twofold serial dilutions of the compounds were prepared from 50 to 1.56 μg/mL and added to the wells containing the biofilms. Plates were incubated again for 48 h at 37 °C and then washed twice with PBS. A measurement of the metabolic activity of the sessile cells was performed using a colorimetric assay with 2*H*-tetrazolium-2,3-bis(2-methoxy-4-nitro-5-sulfophenyl)-5-[(phenylamino)carbonyl] hydroxide salt (X4626, Sigma-Aldrich). Plates were read with a spectrophotometer plate reader set at 492 nm. The MIC was defined as the drug concentration at which the optical density value was equal to or less than 50% of that of the drug-free biofilm.

Electron Microscopy. The *C. albicans* CAF2-1 strain was grown in 10 mL of YNB liquid cultures (50 mL plastic tubes, 37 °C, 2 h). At this time, simplexene D (**9**, 1 mg/mL in DMSO) was added at a concentration of 16 μg/mL, and the cultures were grown during 18 h to evaluate its cytotoxic effect. The samples were centrifuged (10 min, 1300*g*, room temperature), the supernatant was discarded, and the resulting pellet was prepared.[39] Briefly, the pellets were prefixed with a solution of 3% glutaraldehyde−2% paraformaldehyde in 0.07 M phosphate buffer (pH 7), embedded in 2% agarose, and postfixed with a solution of 1% OsO_4. They were then dehydrated in a graduated series of ethanol solutions [30, 50, 70, 95, 100% (v/v)] and embedded in London Resin white resin (14381-UC; London Resin Company). After polymerization for 24 h at 60 °C, thin (0.08 μm) sections were cut and stained with 2% uranyl acetate followed by lead citrate.[40] The thin sections were observed with a transmission electron microscope (Philips CM10) equipped with a Mega View II camera. Controls were performed in the same way without simplexene D (**9**) or with DMSO alone.

■ ASSOCIATED CONTENT

Ⓢ Supporting Information

The Supporting Information is available free of charge on the ACS Publications website at DOI: 10.1021/acs.jnatprod.5b00744.

Antifungal bioautography of the CH_2Cl_2 extract of the roots of *S. simplex*; dereplication table with molecular formula and molecular ion; 1D and 2D NMR of compounds **5**−**12** and **14** (PDF)

■ AUTHOR INFORMATION

Corresponding Author

*Tel: +41 223793641. Fax: +41 223793399. E-mail: emerson.ferreira@unige.ch (E. F. Queiroz).

Notes

The authors declare no competing financial interest.

■ ACKNOWLEDGMENTS

The authors are thankful to the Swiss National Science Foundation for providing financial support for this project, which aims to identify new antifungal compounds of natural origin (grant CR2313_143733 to J.L.W., E.F.Q., D.S., and K.G.) and are thankful to Mrs E. Michellod for her very helpful technical assistance in TEM experiments.

■ REFERENCES

(1) Ostrosky-Zeichner, L.; Casadevall, A.; Galgiani, J. N.; Odds, F. C.; Rex, J. H. *Nat. Rev. Drug Discovery* **2010**, *9*, 719−727.
(2) Beyda, N. D.; Lewis, R. E.; Garey, K. W. *Ann. Pharmacother.* **2012**, *46*, 1086−1096.
(3) Kuhn, D. D. *Curr. Opin. Investig. Drugs* **2004**, *5*, 186−197.
(4) Ramage, G.; Mowat, E.; Jones, B.; Williams, C.; Lopez-Ribot, J. *Crit. Rev. Microbiol.* **2009**, *35*, 340−355.
(5) Rasmussen, T. B.; Givskov, M. *Int. J. Med. Microbiol.* **2006**, *296*, 149−161.
(6) Denning, D. W.; Perlin, D. S. *Future Microbiol.* **2011**, *6*, 1229−1232.
(7) Newman, D. J.; Cragg, G. M. *J. Nat. Prod.* **2007**, *70*, 461−477.
(8) Torke, B. M. *Bot. J. Linn. Soc.* **2007**, *153*, 343−355.
(9) Torke, B. M.; Schaal, B. A. *Am. J. Bot.* **2008**, *95*, 215−228.

DOI: 10.1021/acs.jnatprod.5b00744
J. Nat. Prod. XXXX, XXX, XXX−XXX

(10) Abdel-Kader, M. S.; Bahler, B. D.; Malone, S.; Werkhoven, M. C. M.; Wisse, J. H.; Neddermann, K. M.; Bursuker, I.; Kingston, D. G. I. *J. Nat. Prod.* **2000**, *63*, 1461−1464.
(11) de Marqui, S. R.; Lemos, R. B.; Santos, L. A.; Castro-Gamboa, I.; Cavalheiro, A. J.; Bolzani, V. D.; Silva, D. H. S.; Scorzoni, L.; Fusco-Almeida, A. M.; Mendes-Giannini, M. J. S.; Young, M. C. M.; Torres, L. M. B. *Quim. Nova* **2008**, *31*, 828−831.
(12) Francisco, D. A. M.; Vieira, I. J. C.; Braz-Filho, R.; Vieira-da-Motta, O.; Mathias, L. *Rev. Bras. Farmacogn.* **2009**, *19*, 366−369.
(13) Rojas, R.; Bustamante, B.; Ventosilla, P.; Fernadez, I.; Caviedes, L.; Gilman, R. H.; Lock, O.; Hammond, G. B. *Chem. Pharm. Bull.* **2006**, *54*, 278−279.
(14) Schaller, F.; Rahalison, L.; Islam, N.; Potterat, O.; Hostettmann, K.; Stoeckli-Evans, H.; Mavi, S. *Helv. Chim. Acta* **2000**, *83*, 407−413.
(15) CYTED. *Plantas Medicinales Iberoamericanas*; Edición de la Organizacion Del Convenio Andrés Bello: Bogota, 2008; p 1003.
(16) Schultes, R. E. *J. Ethnopharmacol.* **1979**, *1*, 79−87.
(17) Borel, C.; Gupta, M. P.; Hostettmann, K. *Phytochemistry* **1987**, *26*, 2685−2689.
(18) Favre-Godal, Q.; Dorsaz, S.; Queiroz, E. F.; Conan, C.; Marcourt, L.; Wardojo, B. P. E.; Voinesco, F.; Buchwalder, A.; Gindro, K.; Sanglard, D.; Wolfender, J. L. *Phytochemistry* **2014**, *105*, 68−78.
(19) Guillarme, D.; Nguyen, D. T. T.; Rudaz, S.; Veuthey, J. L. *Eur. J. Pharm. Biopharm.* **2008**, *68*, 430−440.
(20) Guillarme, D.; Nguyen, D. T. T.; Rudaz, S.; Veuthey, J. L. *Eur. J. Pharm. Biopharm.* **2007**, *66*, 475−482.
(21) Buckingham, J. E. *Dictionary of Natural Products on DVD [Ressource electronique]*; CRC Press: Boca Raton, FL, 2013; p 1, DVD-ROM+.
(22) Kind, T.; Fiehn, O. *BMC Bioinf.* **2007**, *8*, 105.
(23) Orphelin, B.; BrumBousquet, M.; Tillequin, F.; Koch, M.; Moretti, C. *Heterocycles* **1996**, *43*, 173−183.
(24) Jewers, K.; Coker, R. D.; Dougan, J. M.; Sandberg, F. *Phytochemistry* **1971**, *10*, 2263−2265.
(25) Magalhaes, A. F.; Tozzi, A. M. G. A.; Santos, C. C.; Magalhaes, E. G. *J. Nat. Prod.* **2005**, *68*, 1290−1292.
(26) Challal, S.; Queiroz, E. F.; Kloeti, W.; Debrus, B.; Guillarme, D.; Wolfender, J. L. *Planta Med.* **2015**, DOI: 10.1055/s-0035-1545912.
(27) Santos, C. C.; Magalhaes, E. G.; Magalhaes, A. F. *Phytochem. Anal.* **2007**, *18*, 484−488.
(28) Favre-Godal, Q.; Queiroz, E. F.; Wolfender, J.-L. *J. AOAC Int.* **2013**, *96*, 1175−1188.
(29) Tudela, J. L. R.; Donnelly, J. P.; Arendrup, M. C.; Arikan, S.; Barchiesi, F.; Bille, J.; Chryssanthou, E.; Cuenca-Estrella, M.; Dannaoui, E.; Denning, D.; Fegeler, W.; Gaustad, P.; Lass-Florl, C.; Moore, C.; Richardson, M.; Schmalreck, A.; Velegraki, J. A.; Verweij, P. *Clin. Microbiol. Infect.* **2008**, *14*, 982−984.
(30) Pierce, C. G.; Uppuluri, P.; Tristan, A. R.; Wormley, F. L., Jr.; Mowat, E.; Ramage, G.; Lopez-Ribot, J. L. *Nat. Protoc.* **2008**, *3*, 1494−1500.
(31) Frisch, M. J.; Trucks, G. W.; Schlegel, H. B.; Scuseria, G. E.; Robb, M. A.; Cheeseman, J. R.; Scalmani, G.; Barone, V.; Mennucci, B.; Petersson, G. A.; Nakatsuji, H.; Caricato, M.; Li, X.; Hratchian, H. P.; Izmaylov, A. F.; Bloino, J.; Zheng, G.; Sonnenberg, J. L.; Hada, M.; Ehara, M.; Toyota, K.; Fukuda, R.; Hasegawa, J.; Ishida, M.; Nakajima, T.; Honda, Y.; Kitao, O.; Nakai, H.; Vreven, T.; Montgomery, J. A.; Peralta, J. E.; Ogliaro, F.; Bearpark, M.; Heyd, J. J.; Brothers, E.; Kudin, K. N.; Staroverov, V. N.; Kobayashi, R.; Normand, J.; Raghavachari, K.; Rendell, A.; Burant, J. C.; Iyengar, S. S.; Tomasi, J.; Cossi, M.; Rega, N.; Millam, J. M.; Klene, M.; Knox, J. E.; Cross, J. B.; Bakken, V.; Adamo, C.; Jaramillo, J.; Gomperts, R.; Stratmann, R. E.; Yazyev, O.; Austin, A. J.; Cammi, R.; Pomelli, C.; Ochterski, J. W.; Martin, R. L.; Morokuma, K.; Zakrzewski, V. G.; Voth, G. A.; Salvador, P.; Dannenberg, J. J.; Dapprich, S.; Daniels, A. D.; Farkas, O.; Foresman, J. B.; Ortiz, J. V.; Cioslowski, J.; Fox, D. J. *Gaussian 09*, Revision A02; Gaussian, Inc: Wallingford, CT, 2009.
(32) Bruhn, T. S. A.; Hemberger, Y.; Bringmann, G. *SpecDis* version 1.61; University of Wuerzburg: Germany, 2013.
(33) Kessner, D.; Chambers, M.; Burke, R.; Agus, D.; Mallick, P. *Bioinformatics* **2008**, *24*, 2534−2536.
(34) Pluskal, T.; Castillo, S.; Villar-Briones, A.; Oresic, M. *BMC Bioinf.* **2010**, *11*, 395.
(35) Pascual, A.; Nieth, V.; Calandra, T.; Bille, J.; Bolay, S.; Decosterd, L. A.; Buclin, T.; Majcherczyk, P. A.; Sanglard, D.; Marchetti, O. *Antimicrob. Agents Chemother.* **2007**, *51*, 137−143.
(36) Rahalison, L.; Hamburger, M.; Hostettmann, K.; Monod, M.; Frenk, E. *Phytochem. Anal.* **1991**, *2*, 199−203.
(37) Rodriquez-Tudela, J. L.; Donnelly, J. P.; Arendrup, M. C.; Arikan, S.; Barchiesi, F.; Bille, J.; Chryssanthou, E.; Cuenca-Estrella, M.; Dannaoui, E.; Denning, D.; Fegeler, W.; Gaustad, P.; Lass-Flörl, C.; Moore, C.; Richardson, M.; Schmalreck, A.; Velegraki, A.; Verweij, P. *Clin. Microbiol. Infect.* **2008**, *14*, 398−405.
(38) Pierce, C. G.; Uppuluri, P.; Tristan, A. R.; Wormley, F. L., Jr.; Mowat, E.; Ramage, G.; Lopez-Ribot, J. L. *Nat. Protoc.* **2008**, *3*, 1494−1500.
(39) Roland, J.; Vian, B. In *Electron Microscopy of Plant Cells*; Hall, C. H., Ed.; Academic Press: London, 1991; pp 1−66.
(40) Reynolds, E. S. *J. Cell Biol.* **1963**, *17*, 208−212.

DOI: 10.1021/acs.jnatprod.5b00744
J. Nat. Prod. XXXX, XXX, XXX−XXX